

INVESTIGATION OF STRUCTURE FORMATION AND TRIBOTECHNICAL PROPERTIES OF STEEL PLASMA COATINGS AFTER CHEMICAL-HEAT TREATMENT AND LIQUID-PHASE IMPREGNATION

Roman MEDIUKH^{*}, Vira MEDIUKH^{*}, Vasyi LABUNETS^{**}
Pavlo NOSKO^{**}, Oleksandr BASHTA^{**}, Irina KONDRATENKO^{*}

^{*}Fratsevich Institute for Problems in Materials Science NAS of Ukraine, Department of Functional Materials for Medical Application,
Krzhizhanovsky Str., 3, 03142, Kyiv, Ukraine

^{**}Aerospace Faculty, Department of Applied Mechanics and Materials Engineering, National Aviation University,
Lubomyr Husar Ave., 1, 03058, Kyiv, Ukraine

roman.mediukh@gmail.com, vira.mediukh@gmail.com, nau12@ukr.net,
nosko_p@ukr.net, oleksandr.bashta@npp.nau.edu.ua, irina.kondratenko@gmail.com

received 26 June 2022, revised 2 September 2022, accepted 6 September 2022

Abstract: The paper is focused on the studies of the microstructure development and physical and mechanical properties of metal-matrix composite coatings based on steel 11Cr18MoWCU deposited using plasma and galvanoplasma methods. The expediency of combining gas-thermal spraying processes of plasma coatings with open porosity up to 16%–18%, with their subsequent thermodiffusion saturation (chromium plating) or liquid-phase impregnation with eutectic alloys of previously applied Ni–B galvanic layer, is shown. The study of the tribotechnical properties of the proposed coatings showed a significant improvement in their performance under conditions of various types of intensive wear, as well as in corrosive environments.

Key words: plasma coatings, steel 11Cr18MoWCU, composite electrolytic coatings, impregnation, galvanic plasma coatings, chemical-thermal treatment, structure formation, wear resistance

1. INTRODUCTION

In the current conditions of industrial production in different branches of industry, the problems of inadequate reliability and durability of machines and mechanisms are of particular importance. The solution to these problems is determined mainly by enhancing the effectiveness of the parts that provide surface protection from various types of contact damage. The formation of heterogeneous surface coatings possessing a specific set of functional properties is the most economically feasible solution to these problems [1–3].

Uvarova [4] and Rinaldi and Ferravante [5] suggest that one of the ways to achieve this goal is to develop a technology for multi-functional heterogeneous coatings by combining different deposition methods, and this would allow the physical, mechanical and operational properties of coatings to be altered pursuant to changes made in the ratio of phase components.

The deposition of protective metallic coatings by thermal spraying is technologically simple and allows the formation of a variety of coatings varying in their composition and purpose. Their thickness may vary in a wide range, which has been reported to be from 0.1 mm to ≥5 mm in the literature [6–12]. The strength of adhesion of such coatings to the substrate is in the range of 20–100MPa, which is usually insufficient for most of the tribotechnical applications. Therefore, they require further heat or chemical-heat treatment (CHT), which promotes high adhesion and formation of

required composition and heterogeneous structure in the surface, thereby significantly improving the coating properties [13–16].

The functional purpose of gas-thermal coatings can be significantly expanded with the use of galvanic plasma coatings (GPCs). The technology of their deposition consists of two stages. The first stage is the pre-deposition of a galvanic interlayer of eutectic composition, such as Ni–B or Fe–B. The second stage is deposition of gas-thermal coating with total porosity up to 16%–24%. Later, when heating such a composition to the temperature of interlayer eutectic transformation, the gas-thermal coating is impregnated with liquid metal melt during liquid-phase sintering [17–21].

In this work, the 11Cr18MoWCU ferritic steel was used as a material for coating. It is able to work in aggressive environments (acidic or alkaline), and is heat-resistant at operating temperatures up to 900 °C. Molybdenum and copper additives in its composition increase resistance to corrosion in acids [22, 23], whereas tungsten promotes heat resistance [24]. Depending on the type of heat treatment, chromium (Cr₂₃C₆), molybdenum (Mo₂C) and tungsten (WC) carbides may form in this steel.

For the impregnation of the plasma coating of the 11Cr18MoWCU steel, a Ni–B composite electrolytic coating (CEC) was used. At the eutectic temperature (1080 °C) it fills the pores of the steel with a Ni–Ni₃B liquid phase. Upon solidification, the eutectic mixture has the structure of a soft nickel matrix with solid Ni₃B particles. This helps to increase the tribotechnical properties of the obtained coatings.

The present work aims to study new steel 11Cr18MoWCu plasma coatings after CHT (chromising) or after impregnation with liquid metal phase Ni–Ni₃B.

In particular, the paper addresses the study of:

- process of such coatings' structure formation,
- phase composition, and
- tribotechnical properties under various conditions of their contact interaction.

2. MATERIALS AND THE METHODS

To conduct the experiment, two fundamentally different series of samples were made, and the abbreviated schemes of their preparation are given below:

1. Substrate of steels 0.45C/0.20C + CEC Ni–B + plasma coating 11Cr18MoWCu + vacuum heat treatment;
2. Substrate of steels 0.45C/0.20C + plasma coating 11Cr18MoWCu + diffusion chromium saturation.

Before spraying, the substrate surface was treated with steel crumbs with a particle size of 0.5–1.0 mm at a pressure of $3.4\text{--}4.0 \times 10^5$ Pa. Such pre-treatment of the surface is necessary to give it a developed relief and energy-active state to improve the adhesion of the coating to the substrate.

The Ni–B CEC were obtained from nickel chloride electrolyte [25] by co-precipitation of nickel with dispersed particles of amorphous boron with a diameter of about 3–5 μm in the concentration of 80 g/L. With such a boron content in the electrolyte, the eutectic composition of CEC Ni–B, with amorphous boron content of 3.5%–4% in it, is achieved. During the subsequent heat treatment at a temperature of 1080–1100 °C, the Ni–Ni₃B eutectic is formed. The coating deposition rate is 70–80 μm/h at a current density of 10 A/m².

The next coating layer was applied by plasma spraying of 11Cr18MoWCu steel. The vacuum heat treatment was performed according to the following regime: heating to 1110 °C, holding for 2–3 min and cooling simultaneously with the furnace. Under such conditions, eutectic melting of CEC occurs and the Ni–Ni₃B metal melt is drawn into the pores due to capillary pressure and good wetting of the 11Cr18MoWCu steel by the liquid phase. As a result of such impregnation, GPC Ni–B+11Cr18MoWCu is formed.

11Cr18MoWCu stainless chromium–molybdenum steel wire with a diameter of 1.6 mm was used for spraying plasma coatings on the steel 0.45C substrate.

Plasma spraying was performed on an UPU-3D machine in air using argon as a transporting and plasma-forming gas. Spraying parameters were changed to ensure adhesion and to obtain the maximum open porosity of the coating, which is appropriate for the further CHT [17]. The optimal parameters of spraying are as follows: I = 450 A, U = 35 V, distance from the plasmatron nozzle to the sample is 140 mm, gas consumption is 21 L/min, and wire feed rate is 1.5–1.7 kg/h.

The porosity of plasma coatings was measured by mercury porosimetry under ISO 15901-1: 2016.

Heat treatment of samples and parts was performed in the laboratory vacuum electric furnace SShVL 1.25/25 at a residual gas pressure of 5×10^{-3} Pa in the temperature range 1080–1100 °C.

Diffusion saturation by chromium was performed in an electric furnace SNOL-2.3.2/13 in containers made of heat-resistant steel Cr18Ni9Ti with a fusible cover of sodium silicate glass, under controlled temperature and duration of the process. Saturation was performed in powder mixture containing (%wt.): 50 – Fe–Cr

(in the ratio 40:60), 47 – Al₂O₃, 3 – NH₄Cl [15].

To determine the Vickers microhardness and thickness of coating (ISO 6507), we used a microhardness tester PMT-3. The microstructure of the coating was studied on standard metallographic samples (sections) after etching in a nital solution (5% HNO₃ + 95% C₂H₅OH) for 5–15 s at T = 20 °C. For microstructural examinations we used an optical microscope MIM-7.

XRD-studies were performed on a DRON-2.0 diffractometer in filtered Co–K_α radiation. Exposure was performed from the surface of the coatings, and to reduce the surface roughness, the samples were polished.

The distribution of elements in the coating was studied using a microanalyser MS-46 'Cameca'. Electronic scanning was performed in the direction perpendicular to the coating.

The adhesion of the coating to the substrate before and after heat treatment was determined by the shear method (see Fig. 1.) The coating is deposited to one-half of the sample (cylinder) surface. The coating-free end of the sample fits into the matrix. So, the coating leans on the end face of the matrix. Adhesion shear strength was calculated as the ratio of the shear load to the area of the coated cylindrical surface.

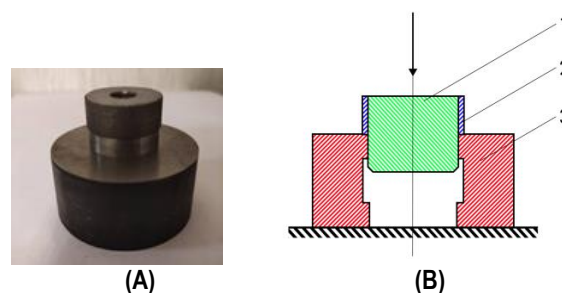


Fig. 1. Device (A) and its scheme (B) for testing of the coating adhesion strength by the shear method: 1 – sample, 2 – coating, 3 – matrix

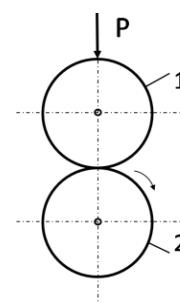


Fig. 2. Scheme of the friction-sliding: 1 – stationary sample with coating, 2 – rotated sample (counterbody)

Tests of coatings' wear resistance under sliding friction were performed on a computerised friction machine 2070 SMT-1 using the disk–disk scheme. Simultaneously, one disk rotated (counterbody), and the other was stationary (see Fig. 2); this simulated friction-sliding. The coating was applied to a stationary disk. Steel 0.45C hardened to HRC 50–52 hardness was used as a counterbody. The sliding speed was constant and equal to 1 m/s, and the specific load was 1 MPa. The tests were performed in air (dry friction) and lubricants TsiATIM-203 and AMG-10 [26] were used. In this case, the 11Cr18MoWCu and Ni–B + 11Cr18MoWCu thermal-spray coating were applied to the generatrix surface of the rings made of 0.45C carbon steel with an outer diameter of 50 mm, an inner diameter of 16 mm and a width of 10 mm. The coated sample was fixed, and the rotating counterbody was made

of 0.45C steel, hardened to a hardness of 48–52 HRC. The tests were performed at a load of 1 MPa and a sliding speed of 1 m/s. The wear rate was determined by the weight reduction method.

Investigations of cavitation-erosion wear of coatings were performed on an installation with a magnetostrictive vibrator at an oscillation frequency of 22 kHz, an amplitude of 40 μm and a distance between the sample and the end of the concentrator of 0.5 mm [27]. The sample weight loss was used as a basis for assessing the wear intensity during 1 h, 2 h and 4 h of tests in a working medium of 5% aqueous solution of HCl at a temperature of 18–20 °C.

Tests of the coatings and the 0.45C steel samples under abrasive wear conditions were performed on samples in the form of plates having a size of 20x15x5 mm. Quartz sand with a particle size of 0.1–0.3 mm was used as an abrasive material. Wear resistance was assessed by the sample weight loss per 1 kg of abrasive powder supplied to the friction area.

Hydroabrasive wear of the coatings was investigated on a hydraulic test rig according to the method described by Burda et al. [28]; as an abrasive material we used quartz sand with a particle size of 0.1–0.3 mm, the concentration of solid particles was 5 wt.% and the pulp flow rate was 30 m/s.

The wear of the samples was determined based on the measured weight loss, which was ascertained using electronic balances VLA-200 with an accuracy of 0.1 mg.

3. RESULTS AND DISCUSSION

Depending on the modes of plasma spraying, a certain porous structure of coatings is created, which is one of their essential characteristics. This can play a positive role, increasing the tribotechnical properties of parts during their operation in the oil, when the pores play the role of oil cups and lubrication grooves. Thus, the microstructure of 11Cr18MoWCu steel plasma coating (Fig. 3A) has a layered structure. The layers mainly consist of particles in the form of thin curved plates and many spherical and irregular round-shaped particles. In Fig. 3C and 3D, there is better visibility of an internal structure of the coating layers, and it is seen that spherical particles are located not only along the boundaries of the layers but also in their middle. The coating has a fairly high porosity. Under the optimal modes of spraying the steel 11Cr18MoWCu, the total porosity of the coating is 20%–24%, and the maximum open porosity is 16%–18%.

According to the microstructure analysis, after chromium plating at a temperature of 1100 °C during 3 h, the coating density increases and the porosity decreases significantly.

The boundaries between the layers and particles become less clear and smoother, the structure becomes more homogeneous (Fig. 3B and 3D) and the coating integrity increases. A chromium coating with a thickness of 10 μm and a hardness of 4–4.5 GPa is formed on the surface. To a depth of 50 μm, the structure of the coating is fine-grained with a microhardness of 8.10 GPa. In the coating towards the substrate one can see thin and narrow layers, which differ significantly in size from the plasma coating without heat treatment and have a microhardness of 4.9 GPa.

Fig. 4 presents the X-ray patterns of plasma coating before (Fig. 4B) and after heat treatment (Fig. 4C). For comparison, the X-ray patterns of 11Cr18MoWCu steel wire (see Fig. 4A) show that it has a ferritic structure, and after spraying (see Fig. 4B) it consists of both austenite and ferrite. The probable explanation for

its formation may be the following. In the process of melting steel at high temperature for a short time there is a complete homogenisation of the alloy. During the subsequent high-speed solidification and high-rate cooling, a high-temperature fine-crystalline phase is formed, firstly austenite, with carbon, chromium, molybdenum, tungsten and copper dissolved in it. This state is thermodynamically unstable at low temperatures, but the driving force of $\gamma \rightarrow \alpha$ transformations is small. Therefore, the very fine grain formed during quenching from the liquid prevents the $\gamma \rightarrow \alpha$ transformation.

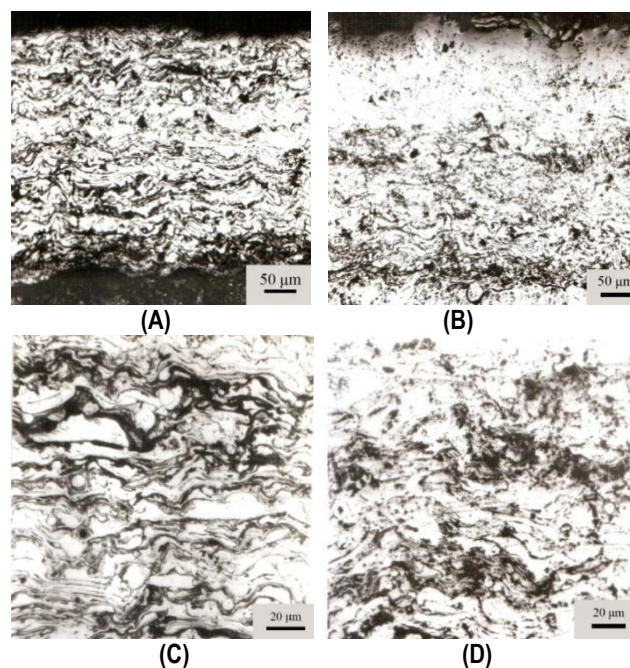


Fig. 3. Microstructure of 11Cr18MoWCu steel plasma coating before (A, C) and after (B, D) CHT chromium plating. (A) and (B) – magnification ×70; (C) and (D) – magnification ×200. CHT, chemical-heat treatment

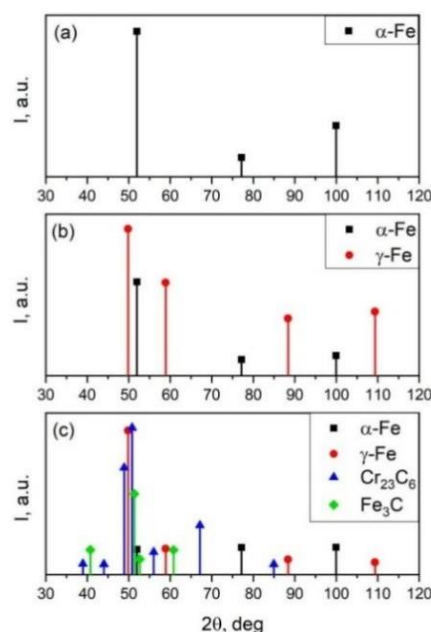


Fig. 4. X-ray patterns: (A) 11Cr18MoWCu steel wire; (B) 11Cr18MoWCu plasma coating before heat treatment; (C) 11Cr18MoWCu plasma coating after CHT chromium plating

Analysis of the bar X-ray pattern of the steel coating after CHT (chromium plating) (see Fig. 4C) showed Fe₃C and Cr₂₃C₆ phase lines' appearance and a decrease in the intensities of the γ -phase lines and an increase in the α -phase. Obviously, during CHT, there is a partial decomposition of the γ -phase into ferrite and the carbide precipitation.

A deeper understanding of the processes that take place during CHT can be obtained by studying the distribution of chemical elements through the thickness of the coating and the transition zone formed by the diffusion of elements and consisting of a solid solution of relevant components. Fig. 5 represents the concentration profiles of Fe and Cr at the boundary of the coating and the substrate after CHT.

Analysis of profiles allows us to make the following conclusions: In the substrate of 0.45C steel the iron content towards the separation surface gradually decreases and the chromium content increases accordingly. A gradual change of concentrations is observed in the area of the steel coating at a distance of up to 10 μ m from the separation surface. The thickness of the transition zone is 18–20 μ m. At greater distances from the transition zone we have a significant deviation from uniformity, and a rapid increase of chromium concentration corresponds to the same sharp drop in iron content. The reason for this is the formation of a concentrated substitutional solid solution of chromium in iron, and thus chromium replaces a portion of iron atoms. Also, chromium carbides may be formed. X-ray structural analysis revealed the inclusions of Cr₂₃C₆ carbide. The width of the peaks on the curves can be used to estimate the dimensions of these inclusions, and it is ascertained that they vary in a range of 3–5 μ m.

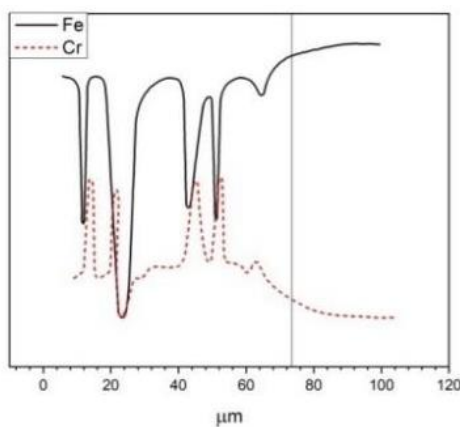


Fig. 5. Profiles of Fe and Cr concentrations at the boundary of 11Cr18MoWCu steel plasma coating and substrate after CHT. The distance from the surface of the coating is plotted along the x-axis. A solid vertical line marks the visible boundary between the coating and the base. The concentration values are given in conventional units. CHT, chemical-heat treatment

The pore size in the plasma coatings is several microns, and their developed surface leads to the formation of a capillary system. The behaviour of capillary system is determined mainly by the properties of the separation margins, specifically their surface energy. Since, to effectively wet the contact surface during further heat treatment and further accelerate the diffusion processes, a liquid phase would be required, it is considered that the impregnation of a structure of coatings characterised by a porous system needs such a phase. Experimental studies of microsections showed that the impregnation of a porous plasma coating with a metal melt of Ni–Ni₃B, with eutectic composition of 20%–25% of

the total coating thickness, provides a dense coating with a characteristic metallic lustre. In addition, melt impregnation fills open pores and cavities between layers of plasma coating (see Fig. 6), and also provides high adhesion to the substrate due to the formation of a transition zone during mutual diffusion of coating and steel substrate elements.



Fig. 6. Microstructure of GPC Ni-B+11Cr18MoWCu after heat treatment at T = 1110 °C, t = 2 min, 500 \times . GPC, galvanic plasma coating

According to the results of experiments, the adhesion of plasma coatings after CHT increases in the order of 1.7 compared to untreated plasma coating (see Fig. 7).

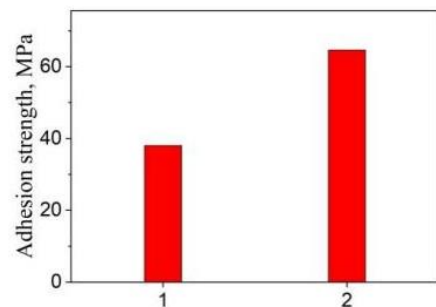


Fig. 7. Adhesion of the plasma coating to the substrate during shear: 1 – as deposited, 11Cr18MoWCu steel; 2 – 11Cr18MoWCu steel after chromium plating

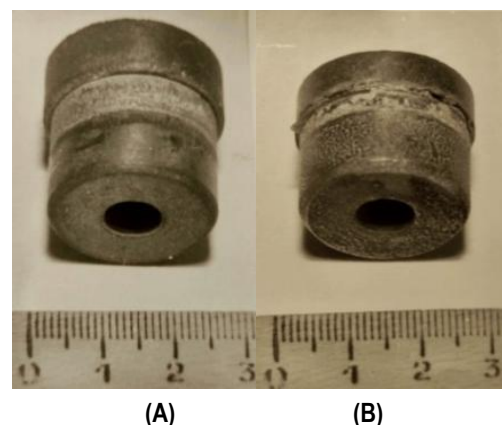


Fig. 8. Samples with plasma coating 11Cr18MoWCu after shear test: (A) as-fabricated; (B) after chromium plating

Figure 8 shows samples with coatings after shear test. As-fabricated plasma coating without CHT (Fig. 8A) is sheared from the substrate, smoothing its rough surface, and the coating after

CHT (Fig. 8B) is cut in the place of mutual diffusion between the coating and the substrate.

11Cr18MoWCu plasma coatings after impregnation with liquid-phase Ni-Ni3B are cut as a solid cast material, which indicates the high strength of adhesion of the GPC to the substrate.

The results of tests under conditions of cavitation-erosion wear (see Fig. 9) showed a slight increase in the stability of carbon steels 0.20C and 0.45C after plasma spraying (curves 3 and 4).

Additionally, due to insufficient adhesion of the coating to the substrate and the presence of a zone with high concentration of defects between them, the coating sometimes delaminates.

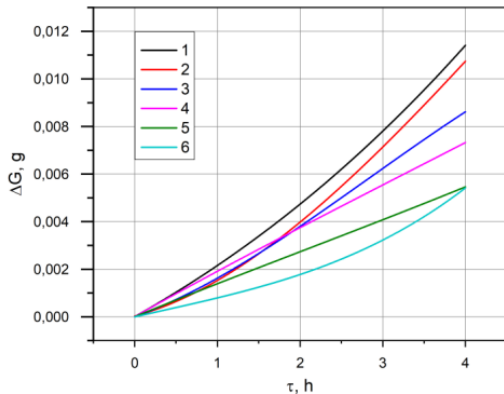


Fig. 9. Dependence of weight loss (ΔG) of 0.20C steel (curves 1, 3, 6) and 0.45C steel (curves 2, 4, 5) in cavitation-erosion wear: 1, 2 – without coating; 3, 4 – with plasma coating; 5, 6 – with plasma coating after CHT. CHT, chemical-heat treatment

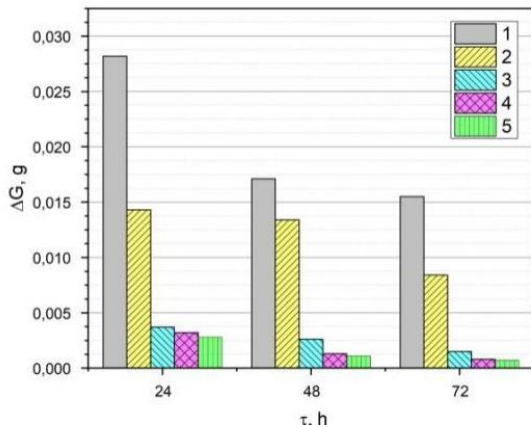


Fig. 10. Dependence of weight loss (ΔG) on the tests' duration (τ) in corrosion-abrasive wear of 11Cr18MoWCu steel plasma coating before and after CHT and impregnation with liquid eutectic phase Ni-Ni3B: 1 – standard 0.45C steel; 2 – plasma coating; 3 – plasma coating after CHT; 4 – plasma coating after impregnation; 5 – plasma coating after CHT and impregnation. CHT, chemical-heat treatment

Thermodiffusion chromium plating of plasma coatings significantly reduces porosity, and heals a defective transition zone with the formation of a transition layer between the coating and substrate, which increases the protective properties of such coatings (see Fig. 9, curves 5 and 6). Studies show that plasma coatings after CHT are 1.5 times superior to untreated coating and, accordingly, 2 times superior to the uncoated 0.20C and 0.45C steels under conditions of cavitation-erosion wear.

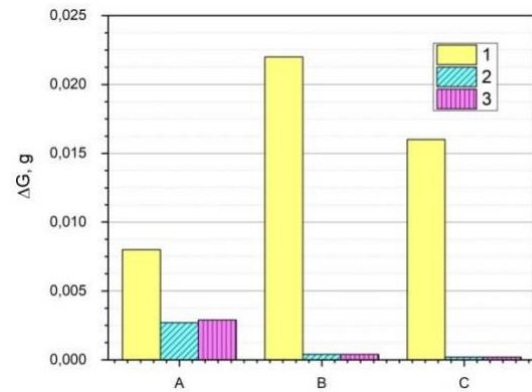


Fig. 11. Dependence of weight loss (ΔG) of the standard 0.45C steel (A), plasma coating 11Cr18MoWCu (B) and GPC Ni-B + 11Cr18MoWCu (C) under sliding friction conditions: 1 – dry friction; 2 – in TslATIM-203 oil; 3 – in AMG-10 oil. GPC, galvanic plasma coating

Studies of coatings under conditions of corrosion and abrasive wear have shown (see Fig. 10) that steel plasma coatings after different types of heat treatment have much better results compared to the standard 0.45C steel, especially after 72 h of testing, and five times less wear than as-fabricated coating.

The results of friction and wear studies showed high wear resistance of plasma coatings 11Cr18MoWCu and GPC Ni-B + 11Cr18MoWCu, especially in lubricants (see Fig. 11). Coatings running-in effectively resist the phenomena of adhesion and have a high relaxation ability.

4. CONCLUSIONS

Research into the features of structure formation and tribotechnical properties of composite 11Cr18MoWCu steel plasma and galvanoplasmic coatings showed the feasibility of combining the processes of gas-thermal spraying of plasma coatings with open porosity up to 16%–18% and liquid phase of the eutectic composition of the pre-applied Ni-B galvanic layer.

The technology of combined steel plasma coating deposition is proposed. It is proved that after chromium plating at a temperature of 1100 °C and exposure for 3 h, the density of the coating increases, and the number of microcavities in it decreases significantly. The boundaries between the layers and particles become less clear and smoothed, and the structure becomes more homogeneous, increasing the continuity of the coating. Impregnation of porous plasma coatings with the liquid phase of the eutectic composition from the previously applied Ni-B galvanic layer fills open pores and cavities between the layers of the plasma coating with Ni-Ni3B eutectic. The formation of a transition zone as a result of mutual diffusion of the coating and substrate elements contributes to a significant increase in adhesion.

Investigation of physical and mechanical properties of the studied coatings showed a significant improvement in their performance under different types of wear and corrosive environments.

The results of experimental tests prove the following indications concerning plasma coatings after CHT: In conditions of cavitation-erosion wear, it is 1.5 times superior to as-fabricated coating, and 2 times superior to the results obtained when the uncoated 0.20C and 0.45C steel are used; under conditions of

corrosion-abrasive wear, it yields much better results than those obtained with standard 0.45C steel, especially after 72 h of testing, and five times less wear than plasma coating without heat treatment.

REFERENCES

1. Hetmanczyk M, Swadzba L, Mendala B. Advanced Materials and Protective Coatings in Aero-Engines Application. *Journal of Achievements in Materials and Manufacturing Engineering*. 2007; 24(1):372–81.
2. Uvarova I, Babutina T, Kostenko V, Cavyak M. From Nanophased Powders to Composite Coatings. *Functional Materials*. 2001;8(1): 185–8.
3. Vijayanand P, Kumar A, Vijaya Kumar KR, Vinod A, Kumaran P, Arungalai Vendan S. Characterizations of Plasma Sprayed Composite Coatings Over 1020 Mild Steel. *Journal of Mechanical Science and Technology*. 2017;31(10):4747–54.
4. Uvarova I. Ultrafine and Nanophased Powders as the Fillers in Composite Coatings. *Journal of Advanced Materials*. 2000 Apr; 32(2):26–31.
5. Rinaldi C, Ferravante L. An Innovative Shrouded Plasma Technique Producing Clean Coatings with Good Hot Corrosion Resistance for Gas Turbine Blades. *EUROMAT 2001 Conf. Proc. Rimini*. 2001.
6. Gill BJ, Ridding FL. Argon Shrouded Plasma Spray Technology for Production Applications. *Surface Engineering*, 1986;2(3):169–76.
7. Brezinová J, Guzanová A, Draganovská D, Egri M. Assessment Tribological Properties of Coatings Applied by HVOF Technology. *Acta Mechanica et Automatica*. 2013 Sep 1;7(3):135–9.
8. Fauchais P, Vardelle M. Understanding the Formation of D.C. Plasma Sprayed Coatings. *Materials Science Forum*. 2003 Aug;426–432:2459–66.
9. Coddet C, Verdy C, Dembinski L, Grosdidier T, Cornu D, Garcia JC. High Properties Metallic Alloys Obtained through the Thermal Spray Route. *Materials Science Forum*. 2003 Aug;426–432:2467–72.
10. Hardwicke CU, Lau Y-C. Advances in Thermal Spray Coatings for Gas Turbines and Energy Generation: A Review. *Journal of Thermal Spray Technology*. 2013 Feb 28;22(5):564–76.
11. Thorpe ML. Thermal Spray, Industry in Transition. *Advanced Mat. and Proc.* 1993;143(5):50–61.
12. Bresinova J, Gubanova F, Draganovska D, Marushchak PO, Landovala M. Spray Coatings Containing WC and WB Particles. *Acta Mechanica et Automatica*. 2016;10(4):296–299.
13. Smagorinski ME, Tsantrizos PG. Sprayed Metals and their Thermal Treatment. *EUROMAT 2001 Conf. Proc. Rimini*. 2001.
14. Kabatova M, Medukh R, Kostenko V, Mihalik J, Seveikova J. Improvement of Corrosion and Wear Resistance of Sintered Steels by Coatings. In Vienna; 2004. p. 423–6.
15. Medyukh RM, Medyukh VK, Uvarova IV. Diffusion Chromizing of Molybdenum-Based Plasma Coatings. *Powder Metallurgy and Metal Ceramics*. 2018 Jan;56(9–10):535–40.
16. Staia MH, Ramos E, Carrasquero A, Roman A, Lesage J, Chicot D, et al. Effect of substrate roughness induced by grit blasting upon adhesion of WC-17% Co thermal sprayed coatings. *Thin Solid Films*. 2000 Dec;377–378:657–64.
17. Guslienko Yu, Mediukh R, Tikhonovich T, Chudovskiy V, Pavlenko N. Structure and Wear Resistance of Composite Galvanoplasma Coatings. *Powder Metallurgy*. 1989;1:31–4.
18. Guslienko Yu, Kostenko V, Medukh R, Uvarova I, Kabatova M, Dzubinsky M, Dudrova E. Structure and Properties of Boride Composite Coatings. *Functional Materials*. 2001;8(1):193–5.
19. Meidukh R, Kabatova M, Parilak L, Kostenko V, Dzubinsky M, Dudrova E. Microstructure and Properties of Ni-B and Ni-B-WC Coating Layers on Sintered Steels. 11 Int. Symposium of Metallography. Slovak Republic; 2001. p. 536–8.
20. Medukh R, Kabatova M, Parilak L, Kostenko V, Dzubinsky M, Dudrova E. Microstructure and Properties of Layers Produced on Sintered Steels by Electrolytic Coatings and Diffusion Chroming. Int. Conference "Protective Coating 2002". Slovak Republic; 2002.
21. Odhiambo JG, Li W, Zhao Y, Li C. Porosity and Its Significance in Plasma-Sprayed Coatings. *Coatings*. 2019 Jul 23;9(7):460.
22. Yang B, Shi C, Li Y, Lei Q, Nie Y. Effect of Cu on the corrosion resistance and electrochemical response of a Ni-Co-Cr-Mo alloy in acidic chloride solution. *Journal of Materials Research*. 2018 Oct 2;33(22):3801–8.
23. Hou Y, Li Y, Wang F, Zhang C, Koizumi Y, Chiba A. Influence of Mo concentration on corrosion resistance to HF acid solution of Ni-Co-Cr-Mo alloys with and without Cu. *Corrosion Science*. 2015 Oct;99:185–93.
24. Jung S, Jeon C, Jo YH, Choi W-M, Lee B-J, Oh Y-J, et al. Effects of tungsten and molybdenum on high-temperature tensile properties of five heat-resistant austenitic stainless steels. *Materials Science and Engineering: A*. 2016 Feb;656:190–9.
25. Guslienko Y, Luchka M, Savakin V, Buray M. Patent of Ukraine. 1283, 28.02.1997.
26. Pašečko M, Kindačuk MV, Labunec' VF, Dziedzic K, Rad'ko OV, Korbut ĘV. *Tribologia*. Lublin: Politechnika Lubelska; 2017.
27. Kluk A, Medukh R, Nekož A, Stetsishin M, Dzub A. Increasing of Cavitation-Erosion Resistance of Carbon Steels by Plasma Spraying and Subsequent Thermal-Diffusion Chromium Plating. *Problems of Frictions and Wear*. 1987;31:66–8.
28. Burda M, Dovzinskiy I, Burda Yu. Patent of Ukraine. 92234, 11.10.2010.

Roman Mediuk:  <http://orcid.org/0000-0003-2176-9321>

Vira Mediukh:  <http://orcid.org/0000-0003-1592-193X>

Vasyl Labunets:  <http://orcid.org/0000-0002-7860-8468>

Pavlo Nosko:  <https://orcid.org/0000-0003-4792-6460>

Oleksandr Bashta:  <https://orcid.org/0000-0001-7914-897X>

Irina Kondratenko:  <http://orcid.org/0000-0001-7970-2248>